molecules

MDPI

Article

NH Stretching Frequencies of Intramolecularly Hydrogen-Bonded Systems: An Experimental and Theoretical Study

Poul Erik Hansen [1,*], Mohammad Vakili [2], Fadhil S. Kamounah [3] and Jens Spanget-Larsen [1,*]

[1] Department of Science and Environment, Roskilde University, Universitetsvej 1, DK-4000 Roskilde, Denmark
[2] Department of Chemistry, Faculty of Science, Ferdowsi University of Mashhad, Mashhad 91775-1436, Iran; vakili-m@um.ac.ir
[3] Department of Chemistry, University of Copenhagen, Universitetsparken 5, DK-2100 Copenhagen, Denmark; fadil@chem.ku.dk
* Correspondence: poulerik@ruc.dk (P.E.H.); spanget@ruc.dk (J.S.-L.); Tel.: +45-4674-2432 (P.E.H.); +45-4674-2710 (J.S.-L.)

Abstract: The vibrational NH stretching transitions in secondary amines with intramolecular NH···O hydrogen bonds were investigated by experimental and theoretical methods, considering a large number of compounds and covering a wide range of stretching wavenumbers. The assignment of the NH stretching transitions in the experimental IR spectra was, in several instances, supported by measurement of the corresponding ND wavenumbers and by correlation with the observed NH proton chemical shifts. The observed wavenumbers were correlated with theoretical wavenumbers predicted with B3LYP density functional theory, using the basis sets 6-311++G(d,p) and 6-31G(d) and considering the harmonic as well as the anharmonic VPT2 approximation. Excellent correlations were established between observed wavenumbers and calculated harmonic values. However, the correlations were non-linear, in contrast to the results of previous investigations of the corresponding OH···O systems. The anharmonic VPT2 wavenumbers were found to be linearly related to the corresponding harmonic values. The results provide correlation equations for the prediction of NH stretching bands on the basis of standard B3LYP/6-311++G(d,p) and B3LYP/6-31G(d) harmonic analyses, with standard deviations close to 38 cm^{-1}. This is significant because the full anharmonic VPT2 analysis tends to be impractical for large molecules, requiring orders of magnitude more computing time than the harmonic analysis.

Keywords: secondary amines; NH stretching wavenumbers; NH/ND isotopic wavenumber ratios; NMR chemical shifts; DFT calculations; anharmonicity

check for updates

Citation: Hansen, P.E.; Vakili, M.; Kamounah, F.S.; Spanget-Larsen, J. NH Stretching Frequencies of Intramolecularly Hydrogen-Bonded Systems: An Experimental and Theoretical Study. *Molecules* **2021**, *26*, 7651. https://doi.org/10.3390/molecules26247651

Academic Editor: Boris A. Kolesov

Received: 12 November 2021
Accepted: 13 December 2021
Published: 17 December 2021

Publisher's Note: MDPI stays neutral with regard to jurisdictional claims in published maps and institutional affiliations.

Copyright: © 2021 by the authors. Licensee MDPI, Basel, Switzerland. This article is an open access article distributed under the terms and conditions of the Creative Commons Attribution (CC BY) license (https://creativecommons.org/licenses/by/4.0/).

1. Introduction

It is well known that hydrogen-bonded linkages play major roles in a variety of areas in chemistry and molecular biology, and the investigation of such linkages by spectroscopic procedures is a subject of current interest [1]. Historically, IR absorption spectroscopy has been the most important spectroscopic tool in the investigation of hydrogen-bonded systems, typically involving OH···O and NH···O linkages [2–4]. The corresponding OH and NH stretching frequencies are thus indicative of the hydrogen bond strength [5]. However, the assignment of these bands in the measured IR spectra is frequently difficult because of overlap with signals due to traces of water or CH stretching vibrations. In systems with strong hydrogen bonds, the situation is further complicated by the influence of anharmonic effects, leading to band broadening and distribution of the intensity associated with the OH or NH stretching motion over several vibrational modes. In many cases, a specific OH or NH stretching band may be difficult to identify in the experimental IR spectrum [6–10].

The possibility to predict the vibrational transitions of hydrogen-bonded systems by theoretical methods has been of interest for decades [11]. Today, advanced procedures

such as coupled-cluster (CCSD(T)) calculations can predict vibrational wavenumbers for small molecules within 10 cm^{-1} of the experimental values [12]. However, this level of theory is not feasible for large molecules, and in general, approximate methods must be applied. Most calculations of vibrational frequencies are performed within the harmonic approximation [13,14]. Scott and Radom [14] and Wong [15] investigated the harmonic vibrational frequencies obtained by a variety of calculational procedures for a large test set of molecular vibrations. They found that density functional theories (DFT) [13,16] such as B3LYP [17,18] and B3PW91 [17,19] led to the most successful correlations between observed and calculated vibrational wavenumbers. With a modest basis set such as 6-31G(d) and using a semiempirical scale factor close to 0.96, the application of these procedures resulted in an overall root-mean-square (RMS) error equal to 34 cm^{-1} [14,15]. Harmonic wavenumbers calculated by DFT procedures (in particular B3LYP) have thus been used to support the vibrational assignments in numerous IR spectroscopic investigations.

However, as indicated above, the harmonic approximation tends to fail for strongly hydrogen-bonded systems. A study was performed some time ago of a series of OH···O systems including weak, strong, and very strong intramolecular hydrogen bonds, with OH stretching wavenumbers ranging from 3600 to 1900 cm^{-1} [20,21]. Standard B3LYP harmonic analyses with the usual scale factors led to the prediction of too large OH stretching wavenumbers for systems with strong and short hydrogen bonds, evidently due to lowering of the wavenumbers by anharmonic effects. On the other hand, application of the VPT2 anharmonic approximation developed by Barone et al. [22,23] overestimated the anharmonic lowering of the OH stretching wavenumbers, leading to predictions of much too low wavenumbers for strong hydrogen bonds, for example, almost 900 cm^{-1} too low for nitromalonamide enol with B3LYP/6-31G(d) and more than 1000 cm^{-1} too low for dibenzoylmethane enol with B3LYP/cc-pVDZ [20,21,24,25]. Fortunately, a satisfactory linear correlation was established between observed OH stretching wavenumbers and calculated harmonic values in the complete experimental range from 3600 to 1900 cm^{-1}, thereby enabling a convenient prediction of effective OH stretching band centers from the results of a standard harmonic analysis [20,21].

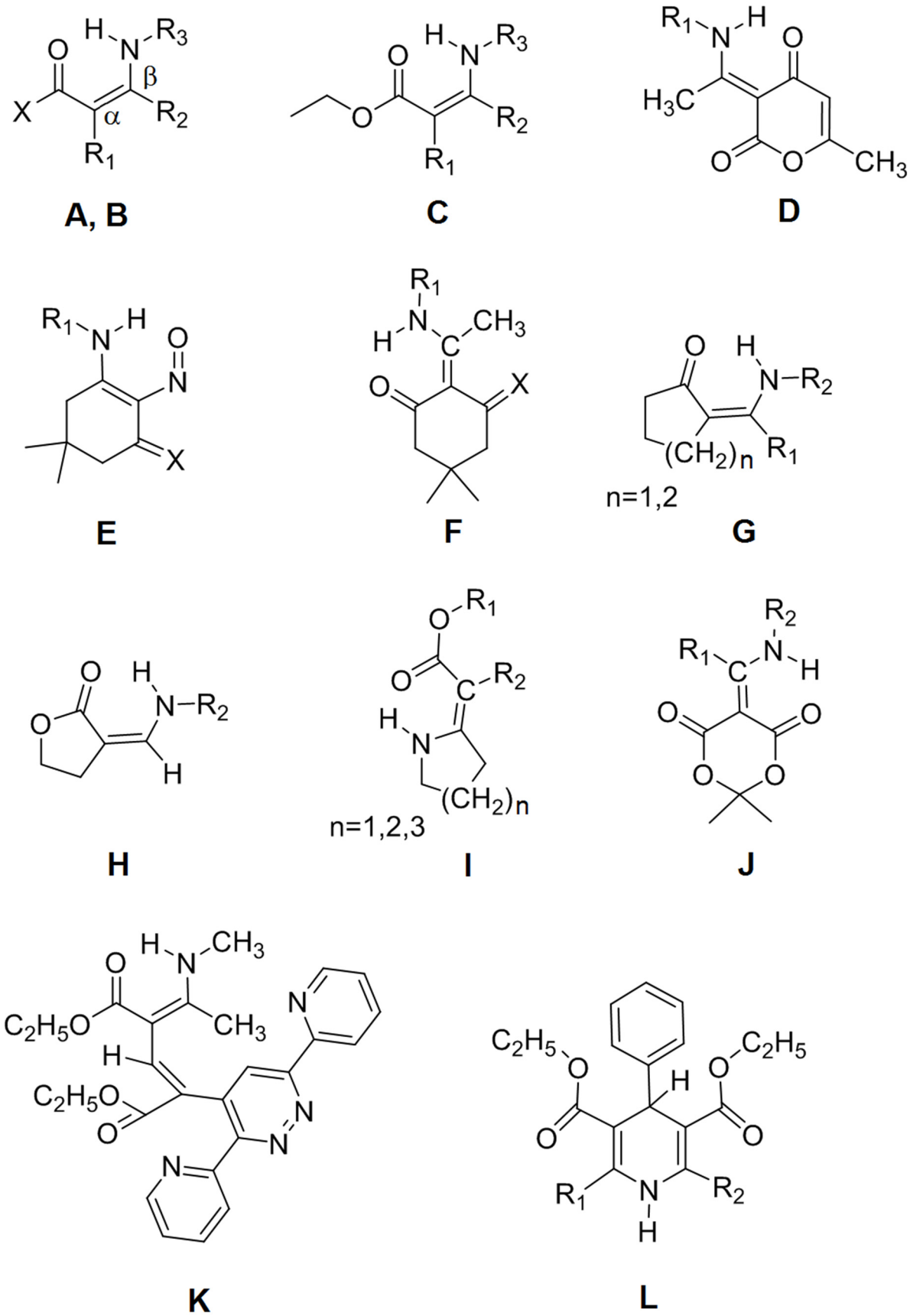

Scheme 1. General structures of the investigated compounds. For substituents and names, see Table 1.

Table 1. The compounds investigated in this study (for type, etc., see Scheme 1).

No.	Type	R_1	R_2	R_3	X	Name
1	A	H	H	*t*-Butyl	H	(*Z*)-3-(tert-butylamino)acrylaldehyde
2	A	H	H	Ethyl	CH_3	(*Z*)-4-(ethylamino)but-3-en-2-one
3	A	H	H	Ethyl	CF_3	(*Z*)-4-(ethylamino)-1,1,1-trifluorobut-3-en-2-one
4	A	CH_3	H	CH_3	CF_3	(*Z*)-1,1,1-trifluoro-3-methyl-4-(methylamino)but-3-en-2-one
5	A	H	NO_2	CH_3	CH_3	(*E*)-4-methylamino-4-nitrobut-3-en-2-one
6	B	H	CH_3	Ph (phenyl)	CH_3	(*Z*)-4-(phenylamino)pent-3-en-2-one
7	B	H	CH_3	*p*-ClPh	Ph	(*Z*)-3-(4-chlorophenylamino)-1-phenylbut-2-en-1-one
8	B	H	CH_3	*o*-CH_3Ph	CH_3	(*Z*)-4-(o-tolylamino)pent-3-en-2-one
9	B	H	CH_3	*o*-FPh	CH_3	(*Z*)-4-(2-fluorophenylamino)pent-3-en-2-one
10	B	H	CH_3	*o*-ClPh	CH_3	(*Z*)-4-(2-chlorophenylamino)pent-3-en-2-one
11	B	H	CH_3	2,6-diCH_3Ph	CH_3	(*Z*)-4-(2,6-dimethylphenylamino)pent-3-en-2-one
12	B	H	CH_3	CH_3	CH_3	(*Z*)-4-(methylamino)pent-3-en-2-one
13	B	H	Ph	Isopropyl	CF_3	(*Z*)-1,1,1-trifluoro-4-(isopropylamino)-4-phenylbut-3-en-2-one
14	B	CH_3	CH_3	CH_3	CH_3	(*Z*)-3-methyl-4-(methylamino)pent-3-en-2-one
15	B	CH_3	CH_3	*p*-OCH_3Ph	CH_3	(*Z*)-4-(4-methoxyphenylamino)-3-methylpent-3-en-2-one
16	C	H	CH_3	Ph	-	(*Z*)-ethyl 3-(phenylamino)but-2-enoate
17	C	H	CH_3	CH_3	-	(*Z*)-ethyl 3-(methylamino)but-2-enoate
18	C	CH_3	CH_3	Ph	-	(*Z*)-ethyl 2-methyl-3-(phenylamino)but-2-enoate
19	C	CH_3	CH_3	CH_3	-	(*Z*)-ethyl 2-methyl-3-(methylamino)but-2-enoate
20	C	CH_3	CH_3	CH_2Ph	-	(*Z*)-ethyl 3-(benzylamino)-2-methylbut-2-enoate
21	C	H	CH_3	CH_2Ph	-	(*Z*)-ethyl 3-(benzylamino)but-2-enoate
22	D	$CH_2CH_2NH_2$	-	-	-	(*E*)-3-(1-(2-aminoethylamino)ethylidene)-6-methyl-2*H*-pyran-2,4(3*H*)-dione
23	D	*p*-CH_3OPh	-	-	-	(*E*)-3-(1-(4-methoxyphenylamino)ethylidene)-6-methyl-2*H*-pyran-2,4(3*H*)-dione
24	D	*p*-ClPh	-	-	-	(*E*)-3-(1-(4-chlorophenylamino)ethylidene)-6-methyl-2*H*-pyran-2,4(3*H*)-dione

Table 1. *Cont.*

No.	Type	R_1	R_2	R_3	X	Name
25	E	*m*-CH_3OPh	-	-	-	5,5-dimethyl-3-(*m*-anisidino)-2-nitroso-2-cyclohexen-1-one
26	E	Ph	-	-	-	5,5-dimethyl-3-anilino-2-nitroso-2-cyclohexen-1-one
27	F	CH_3	-	-	-	5,5-dimethyl-2-(1-(methylamino)ethylidene)cyclohexane-1,3-dione
28	F	Iso-propyl	-	-	-	2-(1-(isopropylamino)ethylidene)-5,5-dimethylcyclohexane-1,3-dione
29	F	Ph	-	-	-	5,5-dimethyl-2-(1-(phenylamino)ethylidene)cyclohexane-1,3-dione
30	G	H	CH_3	-	$n = 1$	(*Z*)-2-((methylamino)methylene)cyclopentanone
31	G	CH_3	CH_3	-	$n = 1$	(*Z*)-2-(1-(methylamino)ethylidene)cyclopentanone
32	G	H	Bu	-	$n = 2$	(*Z*)-2-((butylamino)methylene)cyclohexanone
33	H	CH_3	-	-	-	(*E*)-3-((methylamino)methylene)dihydrofuran-2(3*H*)-one
34	H	Ph	-	-	-	(*Z*)-3-((phenylamino)methylene)dihydrofuran-2(3*H*)-one
35	I	Et	COOEt	-	$n = 1$	diethyl 2-(pyrrolidin-2-ylidene)malonate
36	I	Et	COOEt	-	$n = 2$	diethyl 2-(piperidin-2-ylidene)malonate
37	I	Et	COOEt	-	$n = 3$	diethyl 2-(azepan-2-ylidene)malonate
38	J	CH_3	CH_3	-	-	2,2-dimethyl-5-(1-(methylamino)ethylidene)-1,3-dioxane-4,6-dione
39	J	Et	CH_2COOEt	-	-	ethyl 2-(1-(2,2-dimethyl-4,6-dioxo-1,3-dioxan-5-ylidene)propylamino)acetate
40	K	-	-	-	-	(2*E*,4*Z*)-diethyl 2-(3,6-di(pyridin-2-yl)pyridazin-4-yl)-4-(1-(methylamino)-ethylidene)pent-2-enedioate
41	L	CH_2OCOCH_3	CH_2OCOCH_3	-	-	diethyl 2,6-bis(acetoxymethyl)-4-phenyl-1,4-dihydropyridine-3,5-dicarboxylate
42	L	CH_3	CH_2OCOCH_3	-	-	diethyl 2-(acetoxymethyl)-6-methyl-4-phenyl-1,4-dihydropyridine-3,5-dicarboxylate
43	L	CH_3	CH_3	-	-	diethyl 2,6-dimethyl-4-phenyl-1,4-dihydropyridine-3,5-dicarboxylate

Table 1. *Cont.*

No.	Type	R_1	R_2	R_3	X	Name
44	B	H	CH_3	*p*-PhCOOEt	CH_3	(*Z*)-ethyl 4-(4-oxopent-2-en-2-ylamino)benzoate
45	B	CH_3	CH_3	Ph	CH_3	(*Z*)-3-methyl-4-(phenylamino)pent-3-en-2-one

Table 2. Theoretical NH stretching wavenumbers (cm^{-1}; Harm = harmonic, Anh = VPT2 anharmonic) and NH bond lengths R_{NH} (Å) computed with B3LYP. Observed or estimated wavenumbers ν_{NH} (cm^{-1}) and observed NH proton chemical shifts δ_{NH} (ppm). Entries in italics indicate wavenumbers predicted by Equations (1) and (2).

Compound [1]	6-31G(d)				6-311++G(d,p)		Observed		
	R_{NH}	Harm	Anh	*P(Harm)* [2]	Harm	*P(Harm)* [3]	ν_{NH}	δ_{NH}	Ref.
1	1.0236	3410	3208	*3247*	3424	*3251*	3195	-	[26]
2	1.0224	3404	3176	*3242*	3400	*3232*	3190	-	[27]
3	1.0238	3411	3208	*3248*	3422	*3250*	3222	-	[28]
4	1.0221	3432	3214	*3265*	3441	*3264*	3206	10.21	[29]
5	1.0270	3341	3079	*3182*	3362	*3200*	3180	-	[30]
6	1.0303	3274	2932	*3101*	3244	*3071*	3031 [4,5]	12.48	[31]
7	1.0315	3209	2909	*3001*	3242	*3068*	3056	13.07	[32]
8	1.0305	3266	2973	*3090*	3253	*3082*	3058 [5]	12.34	[33]
9	1.0307	3268	2943	*3093*	3258	*3089*	3063 [5]	12.25	[33]
10	1.0306	3276	-	*3104*	3260	*3091*	3047 [5]	12.42	[33]
11	1.0311	3266	-	*3090*	3274	*3108*	3058 [5]	11.95	[33]
12	1.0263	3342	3052	*3183*	3349	*3188*	3171	10.70	[9]
13	1.0272	3340	-	*3181*	3344	*3183*	3205	11.11	[34]
14	1.0265	3322	-	*3161*	3311	*3149*	3041 [5]	11.86	-
15	1.0322	3226	-	*3030*	3205	*3017*	3004 [4]	-	[35]
16	1.0244	3382	3147	*3223*	3388	*3223*	3254 [4]	10.39	[7]
17	1.0194	3432	3247	*3265*	3469	*3283*	3295	8.46	[7]
18	1.0248	3363	-	*3205*	3360	*3198*	-	-	-
19	1.0199	3442	-	*3272*	3439	*3263*	3262	9.14	-
20	1.0215	3425	-	*3259*	3422	*3250*	3282	9.66 [6]	[36]
21	1.0217	3427	-	*3261*	3442	*3265*	3289 [7]	8.95	[37]
22	1.0377	3138	2782	*2860*	3102	*2843*	2870	14.18	[38]
23	1.0422	3059	2574	*2653*	3022	*2665*	2610	15.60	[38]
24	1.0440	3027	2591	*2551*	2978	*2548*	2602	15.90	[38]
25	1.0424	3050	2574	*2626*	3048	*2728*	2560 [8]	18.41	[38]
26	1.0418	3048	2584	*2619*	3031	*2687*	2340 [8]	18.35	[38]
27	1.0330	3208	2817	*2999*	3181	*2981*	-	13.3	[7]
28	1.0345	3172	2814	*2932*	3140	*2913*	2900 [9]	13.6	[7]
29	1.0386	3124	2743	*2828*	3077	*2792*	2760	15.2	[7]
30	1.0231	3420	-	*3255*	3440	*3263*	-	8.84	[39]

Table 2. *Cont.*

Compound [1]	6-31G(d)				6-311++G(d,p)		Observed		
	R_{NH}	Harm	Anh	*P(Harm)* [2]	Harm	*P(Harm)* [3]	ν_{NH}	δ_{NH}	Ref.
31	1.0245	3367	-	*3209*	3374	*3210*	-	10.26	[40, 41]
32	1.0253	3381	3121	*3222*	3390	*3224*	3160	-	[27]
33	1.0118	3599	-	*3359*	3613	*3362*	3302	6.60	[42]
34	1.0216	3449	-	*3277*	3466	*3281*	3314	9.05	[42]
35	1.0194	3481	-	*3299*	3488	*3296*	3317	9.52	[42]
36	1.0236	3385	-	*3226*	3372	*3209*	3242	10.08	[42]
37	1.0222	3405	-	*3243*	3411	*3241*	3280	8.83	[43]
38	1.0262	3341	-	*3182*	3331	*3170*	3224	11.32	[44]
39	1.0292	3318	-	*3157*	3304	*3142*	3172	11.60	[44]
40	1.0217	3415	-	*3251*	3414	*3244*	3270	-	[45]
41	1.0148	3558	-	*3341*	3559	*3336*	3403	7.7	[46]
42	1.0153	3541	-	*3333*	3551	*3332*	3347	6.6	[46]
43	1.0092	3631	-	*3372*	3636	*3371*	3336	5.6	[46]
44	1.0308	3266	-	*3090*	3237	*3062*	3047 [5]	12.64	[47]
45	1.0322	3226	-	*3030*	3205	*3017*	2975 [5]	13.46	[48]

[1] See Table 1. [2] Wavenumbers predicted by Equation (2). [3] Wavenumbers predicted by Equation (1). [4] Not assigned as NH stretching in the referenced paper. [5] Estimated values (Table 3), not included in the correlation analyses. [6] NMR data from Ref. [36]. [7] Value varies slightly with solvent. [8] Not included in the correlation analyses, see Section 3.1. [9] Approximate.

Table 3. NH and ND stretching wavenumbers, ν_{NH} and ν_{ND} (cm^{-1}), measured in CCl_4 solution. Several ν_{NH} values are estimated on the basis of the ν_{NH}/ν_{ND} ratio (footnote 2).

Compound [1]	ν_{NH}	ν_{ND}
6	3031 [2]	2262
8	3058 [2]	2280
9	3063 [2]	2286
10	3047 [2]	2274
11	3058 [2]	2282
14	3041 [2]	2270
16	3254, 3185 [3]	2403
17	3295	2431
19	3262	2411
20	3259	2409
21	3289	2435
44	3047 [2]	2274 [4]
45	2975 [2]	2220

[1] See Table 1. [2] Estimated from the observed ν_{ND}, assuming ν_{NH}/ν_{ND} = 1.34 (see Section 4). [3] Two bands are observed [7]; the larger wavenumber is used in the correlation analyses. [4] Ref. [48].

In this publication we present the results of a similar investigation of a large number of secondary amines with intramolecular NH···O hydrogen-bonded linkages. This type of linkage has the advantage that a wide range of compounds can be investigated because, in general, systems of the type NH···O=C with an intervening double bond are

not tautomeric, in contrast to the corresponding OH···O=C systems. In those cases where the compounds are tautomeric, the data are not included. The structures and names of the investigated compounds are listed in Scheme 1 and Table 1. The emphasis of our study is on the NH stretching bands of the NH···O linkages, covering wavenumbers in the range 3300–2600 cm^{-1}. The aim is to develop simple correlation tools for the prediction of effective NH stretching wavenumbers for NH···O systems, to be useful in those cases where the NH stretching bands are not easily identified in the experimental spectra.

For the purpose of this investigation, a number of substances were synthesized and measured, but most spectroscopic data are quoted from the literature (Table 2). Vibrational assignments were in several cases supported by the investigation of deuterated compounds (NH hydrogen exchanged with deuterium). Further support was obtained by considering the correlation of NH stretching wavenumbers with ^{1}H amine chemical shifts, following the original suggestion by Dudek [7]. Calculations of vibrational transitions were carried out with the B3LYP functional, using two different basis sets, and were performed both in the standard harmonic approximation and in the anharmonic VPT2 approximation. As we shall show, excellent correlations between observed and calculated NH stretching wavenumbers are obtained, but in contrast to the previous results for OH···O systems [20,21], the correlations are non-linear. Additional information is provided as Supplementary Materials, referred to in the ensuing text as Figures S1–S21.

2. Materials and Methods

2.1. Materials

The following substances were synthesized: **6**, **14**, **16**, **17**, **19**, and **45**. For details and characterization, see Figure S21. Deuterated compounds were prepared by dissolving the substances in CCl_4 with a drop of trimethylamine [48]. After the addition of D_2O (1 cm^3), the mixture was stirred for 24 h, and the organic layer was separated and dried using Na_2SO_4.

2.2. Spectroscopy

The IR spectra of **6**, **8**, **9**, **10**, **11**, **14**, **16**, **17**, **19**, **44**, and **45** and of their deuterated analogs were recorded in the 4000–400 cm^{-1} region with a spectral resolution of 2 cm^{-1} by averaging the results of 10 scans on a PerkinElmer Spectrum 2000 FTIR spectrophotometer (Figures S1–S11). The compounds were measured in KBr tablets and when possible also in CCl_4 solutions. The CCl_4 solutions were dried with Na_2SO_4 to remove traces of water from the samples. An example of the recorded spectra is shown in Figure 1, which displays the absorbance curves for normal and deuterated (*Z*)-ethyl 3-(methylamino)but-2-enoate (**17**) in the range 3800 to 900 cm^{-1}. NMR spectra were recorded on Bruker Ultrashield Plus 500 MHz and Bruker Avance 3 spectrometers using $CDCl_3$ as a solvent. For details and spectra, see Figure S21.

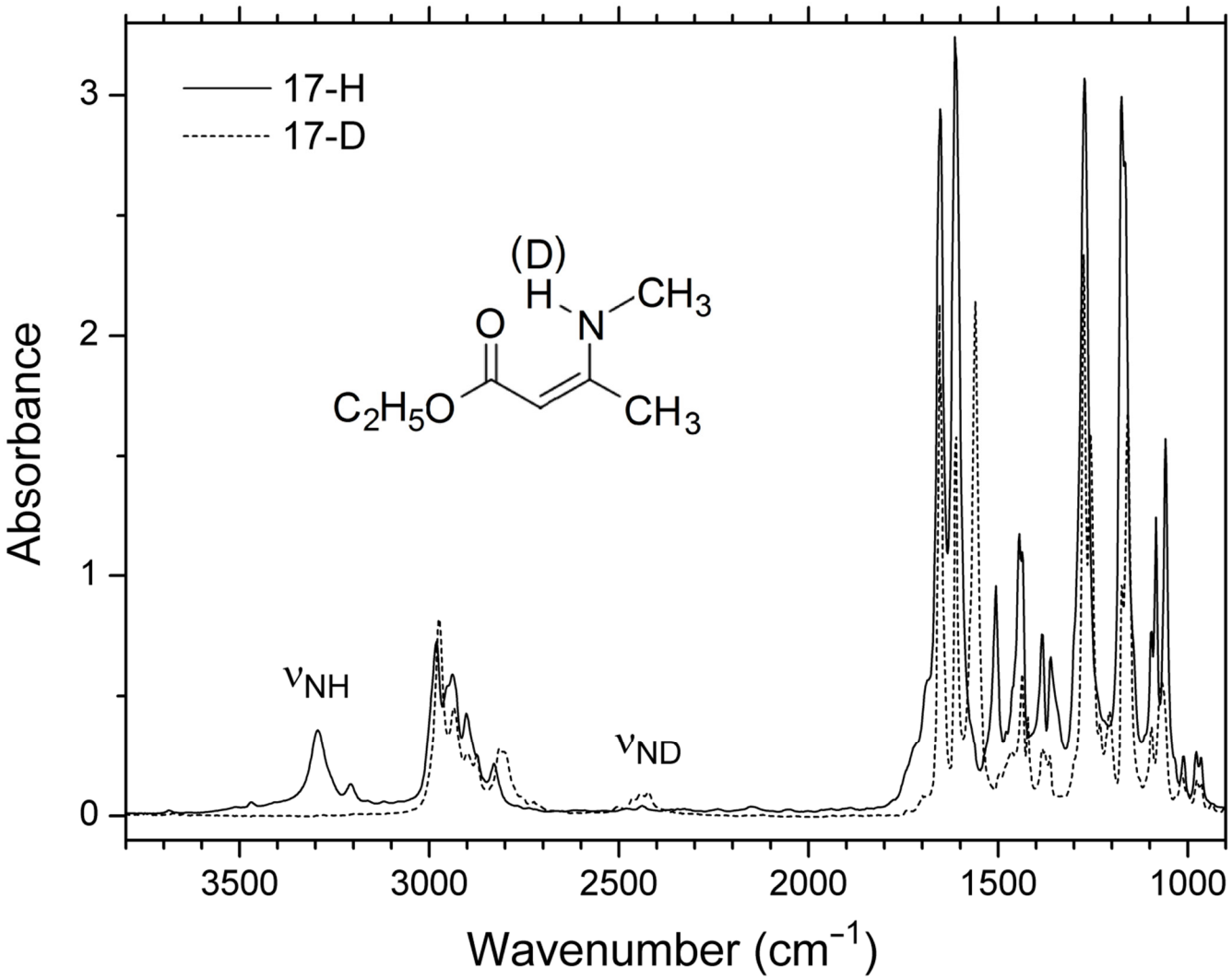

Figure 1. IR spectra of (*Z*)-ethyl 3-(methylamino)but-2-enoate (**17**) measured in CCl_4 solution; 17-H and 17-D indicate the normal and the deuterated compound, respectively. Contributions of 17-H to the 17-D spectrum due to incomplete deuteration are removed by subtraction (Figure S15).

2.3. Calculational Details

Quantum chemical calculations were performed with the Gaussian 09 [49] and the Gaussian 16 [50] software packages producing similar results. Geometry optimizations and standard harmonic analyses were carried out in the gas phase with B3LYP density functional theory (DFT) [17,18] using the basis sets 6-311++G(d,p) and 6-31G(d) [13,49,50]. Several calculations using 6-31G(d) were carried out also with the anharmonic VPT2 approximation [22,23] (freq = anharmonic). The computed NH stretching wavenumbers for the compounds **1**–**45** are listed in Table 2. Detailed listings of results for **17** are provided as Figure S20, considering fundamentals in the range 800–3500 cm^{-1}. For a selection of compounds (**1**, **6**, **16**, **17**, **23**, **29**, and **32**) covering a broad range of NH stretching wavenumbers, additional calculations were performed by using the B3PW91 functional [17,19]. Hydrogen bond energies were estimated using the AIM 2000 software at the B3LYP/6-31G(d) level [51] (Figures S17 and S18).

3. Results

3.1. Experimental NH Stretching Wavenumbers

Measured or estimated NH stretching wavenumbers for the compounds **1**–**45** are listed in Tables 2 and 3. A subset of these compounds, the enaminones, has been thoroughly

investigated by Gilli et al. [38]. NH stretching wavenumbers for the compounds **6, 8, 9, 11, 14, 44,** and **45** were estimated by measuring the IR spectra of the deuterated species and multiplying the observed ND stretching wavenumber with 1.34 (Table 3; see the discussion in Section 4). In these compounds, the NH stretching band appears to be overlapped by the CH stretching bands. The approximate wavenumbers derived in this manner are not included in the correlation analyses.

As a check of the assignments, the experimental NH stretching frequencies are correlated with the observed NH chemical shifts listed in Table 2. The available 26 data points are shown in Figure 2. A non-linear correlation is evident, in contrast to the linear relationships established in the literature, in particular by Dudek [7]. The points for the nitroso compounds **25** and **26** are outliers; they are not included in the correlation analysis (see Section 4). To a good approximation, the remaining 24 points follow an exponential function, leading to RMS standard deviation (SD) = 34.3 cm^{-1} (Figure 2). A similar fit of the data is obtained with a second-order polynomial function, but the exponential function is preferred because of a more satisfactory asymptotical behavior. The correlation equation in Figure 2 can be used to predict NH stretching wavenumbers from the observed chemical shifts.

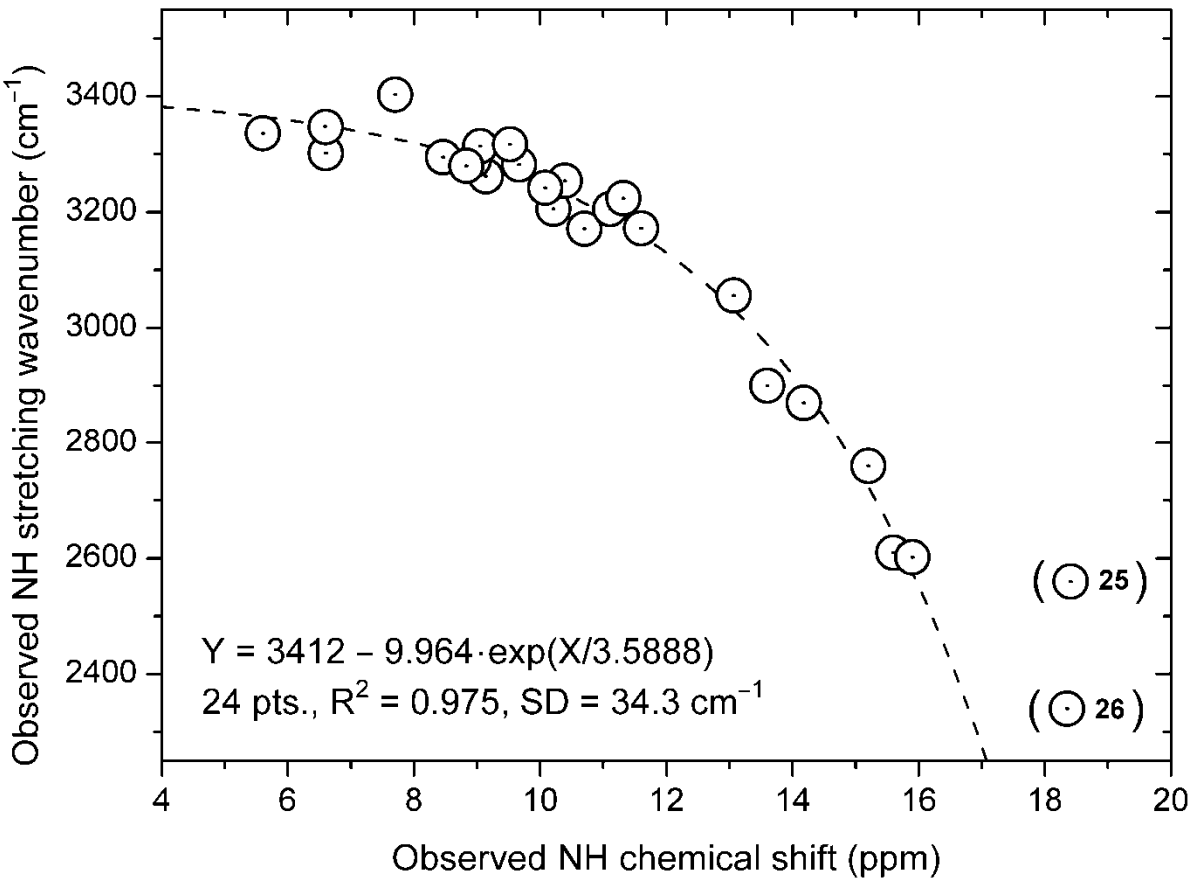

Figure 2. Correlation of observed NH stretching wavenumbers and observed NH chemical shifts. The points for the nitroso compounds **25** and **26** are not included in the correlation analysis.

3.2. Calculations

As pointed out in the Introduction Section, DFT calculations with the B3LYP functional are frequently used to support vibrational assignments in IR spectroscopic investigations. An example is given in Figure 3, which shows the scaling correlation of observed vibrational wavenumbers for the ester **17** and harmonic wavenumbers calculated with B3LYP/6-31++G(d,p), considering all fundamental wavenumbers in the range 800–3500 cm^{-1} (see Figures S19 and S20 for details). A good fit is obtained, even for the NH stretching vibration

observed close to 3300 cm^{-1} (Figure 1, Table 2). The intramolecular hydrogen bond in **17** is weak (Figure S20) and particular anharmonic effects are apparently of minor significance. However, when systems with stronger NH···O hydrogen-bonding are considered, the importance of anharmonic effects increases. Mroginski et al. [52] studied compounds with strong NH···N hydrogen bonds and found that separate scaling of the calculated NH force constants was required in order to reproduce the observed IR bands. Figure 4 shows the correlation of observed NH stretching wavenumbers and calculated harmonic values for the present NH···O linkages, yielding a non-linear correlation that strongly deviates from the linear one in Figure 3. The exponential correlation equation obtained on the basis of the data listed in Table 2 is given in Equation (1):

B3LYP/6-311++G(d,p):

$$P(Harm) = 3509 - 6.310 \times 10^6 \cdot \exp(-\mathrm{Harm}/338.8) \quad (1)$$

(32 points: $R^2 = 0.964$, SD = 38.2 cm^{-1})

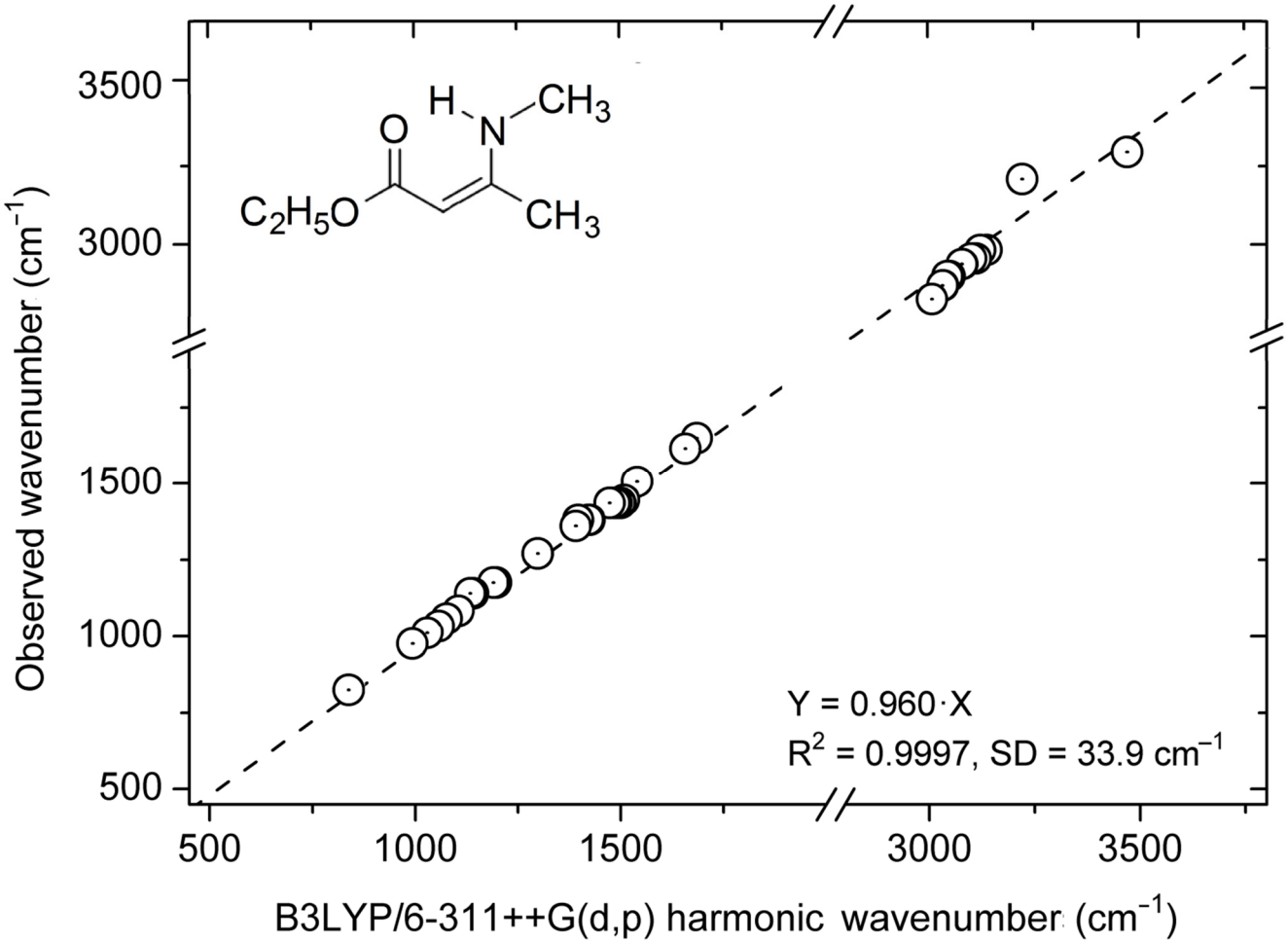

Figure 3. Scaling correlation of observed vibrational wavenumbers for (*Z*)-ethyl 3-(methylamino)but-2-enoate (**17**) and harmonic wavenumbers calculated with B3LYP/6-311++G(d,p) (see Figures S19 and S20 for details).

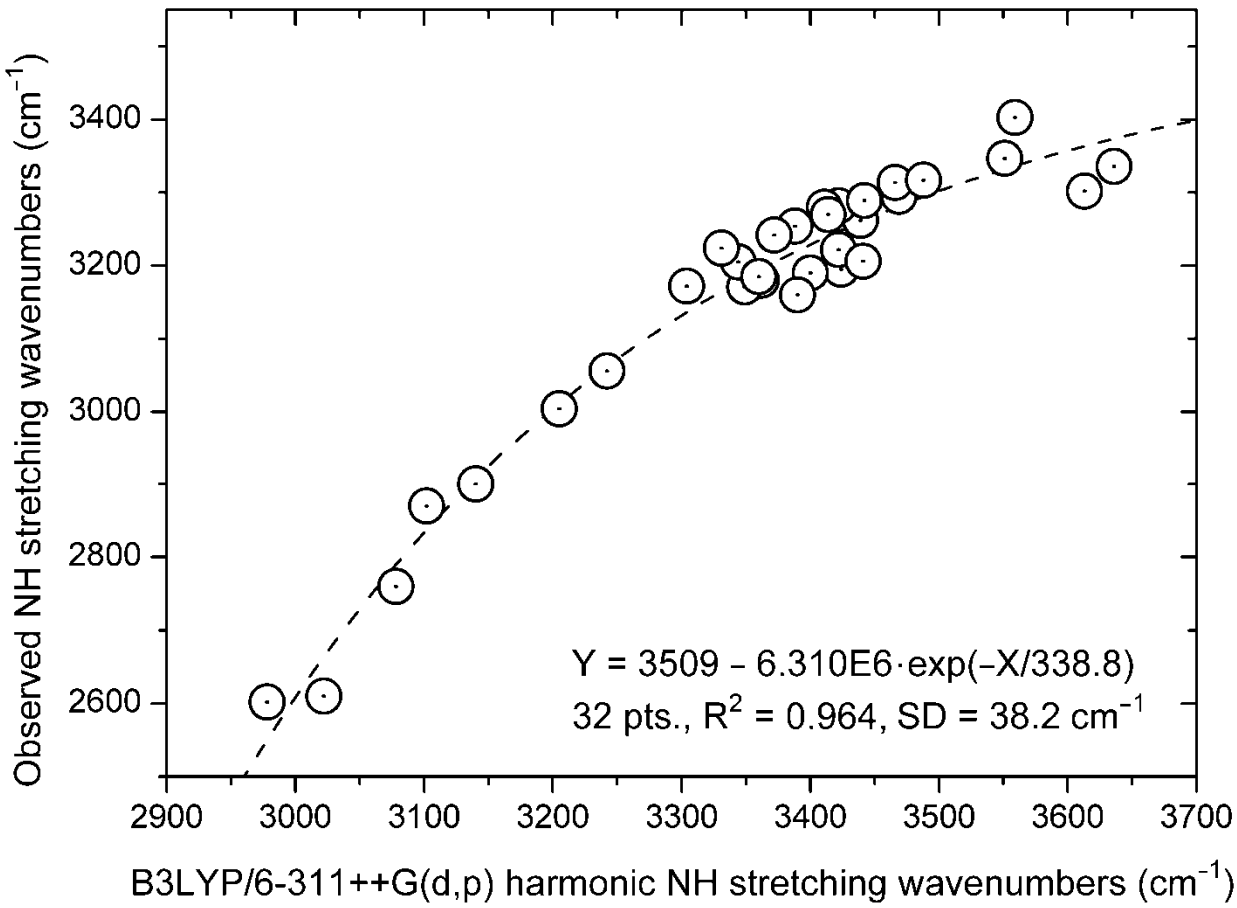

Figure 4. Correlation of observed NH stretching wavenumbers and harmonic wavenumbers calculated with B3LYP/6-311++G(d,p).

Harm is the calculated harmonic wavenumber, and P(Harm) is the value predicted with Equation (1). An SD close to 38 cm^{-1} seems quite acceptable, in view of the uncertainty of many of the experimental wavenumbers and the influence of different environmental effects. Results obtained with the much smaller basis set 6-31G(d) lead to a very similar correlation (Figure S12); the exponential correlation equation is given in Equation (2) as follows:

B3LYP/6-31G(d):

$$P(Harm) = 3470 - 6.714 \times 10^7 \cdot \exp(-\mathrm{Harm}/270.3) \quad (2)$$

(32 points: R^2 = 0.965, SD = 38.1 cm^{-1})

In fact, the wavenumbers obtained with B3LYP/6-31G(d) and B3LYP/6-311++G(d,p) are linearly related with R^2 = 0.991, SD = 15 cm^{-1} (S13). For predictive purposes, the cheaper B3LYP/6-31G(d) procedure is just as efficient as B3LYP/6–311++G(d,p).

The non-linearity of the present correlations is unexpected in view of the previous results for OH···O systems where linear relationships between observed and calculated OH stretching wavenumbers were obtained [20,21]. We carried out VPT2 calculations [22,23] for a series of 21 NH···O species (Table 2), comprising weak as well as strong hydrogen-bonding. However, as shown in Figure S14, the anharmonic NH stretching wavenumbers are essentially linearly related to the harmonic ones (R^2 = 0.986, SD = 27 cm^{-1}) and do not explain the non-linearity of the present correlations. On the other hand, the VPT2 anharmonic wavenumbers are numerically much closer to the experimental values than the harmonic ones, particularly for compounds with strong hydrogen bonds. This is in contrast to the results for OH···O systems, in which the VPT2 approximation significantly underestimated the OH stretching wavenumbers for strongly hydrogen-bonded systems

(see above) [20,21,24,25]. Additional calculations using the B3PW91 functional [17,19] were performed for the compounds **1**, **6**, **16**, **17**, **23**, **29**, and **32**, covering a broad range of NH stretching wavenumbers. The computed harmonic wavenumbers are essentially linearly related to those obtained with B3LYP (R^2 = 0.9999, SD = 2.6 cm^{-1}).

3.3. Structures

The calculated molecular geometries evidently play important roles in the predicted NH stretching wavenumbers for the present NH···O linkages. An excellent linear correlation is observed for calculated wavenumbers and calculated NH bond lengths: R^2 = 0.988, SD = 15 cm^{-1} (Figure S16). Much cruder correlations are found between wavenumbers and N····O and H···O distances. This is similar to the situation observed for OH···O systems [24].

Most of the investigated compounds have substituents with torsional degrees of freedom. In order to estimate the possible influence on the computed NH stretching wavenumber, calculations on several compounds were performed with consideration of different conformations. In general, the influence of the conformation is found to be of minor importance for the calculated wavenumber. For example, as shown in Figure S19, four conformational equilibrium geometries with different energies are located for **17**, but the same NH stretching wavenumber was calculated for all four structures.

The *N*-phenyl groups present in several of the investigated compounds were calculated to be twisted out of the plane of the –NH···O– moieties, and substituents at the phenyl ring were expected to have a minor effect on the NH stretching frequency. This is in agreement with the predicted and observed wavenumbers, except in the case of the observed values for **25** and **26** (see Section 4). Some of the enaminones and enaminoesters may occur both as *E* and *Z* forms, and the ratio between the two may depend on the solvent [39]. These and other points are discussed in the following section.

4. Discussion

NH stretching bands in compounds with weak NH···O hydrogen bonds are generally easy to identify (e.g., Figure 1), but in compounds with stronger hydrogen bonds, the band may be overlapped by CH stretching or other absorption bands. In those cases, deuteration is frequently a good tool. Provided an adequate conversion factor is known, the NH stretching wavenumber (ν_{NH}) can be estimated from the observed ND band (ν_{ND}). The isotope ratio ν_{NH}/ν_{ND} was originally investigated by Novak [53] and more recently by Sobczyk et al. [54], showing a distinct dependence on the NH stretching frequency. However, in both cases, the majority of the data are from intermolecular hydrogen bonds. The intramolecular data reported by Sobczyk et al. [54] are for protonated dimethylaminonaphtalenes, DMANs, quite different from the compounds considered in this paper.

Figure 5 shows a plot of the measured ν_{NH}/ν_{ND} ratios against ν_{ND} for a series of C-type esters with relatively weak hydrogen bonds. These results do not necessarily follow the trends described by Novak [53] and by Sobczyk et al. [54]. The average values of ν_{NH}/ν_{ND} and ν_{ND} for these compounds are about 1.354 and 2400 cm^{-1}, respectively. For the compounds of B type, such as **6, 8, 9, 10, 11**, **14**, **44**, and **45,** the observed values of ν_{ND} are lower (Table 3), amounting to an average close to 2265 cm^{-1}. This indicates stronger hydrogen bonding, and according to the direction suggested by Novak [53], we expect a smaller effective value of the ν_{NH}/ν_{ND} ratio. We shall tentatively assume the value ν_{NH}/ν_{ND} = 1.34 for these compounds, leading to the ν_{NH} wavenumbers listed in Table 3. The wavenumbers obtained in this manner are in the range 2975–3063 cm^{-1} (they are not included in the correlation analyses). This prediction supports the assumption that these NH stretching bands are overlapped by absorption due to CH stretching transitions. The predicted wavenumbers are consistent with the observed NH chemical shifts close to 12 ppm (Table 2), indicating wavenumbers around 3100 cm^{-1} according to the correlation

in Figure 2. They are also in good agreement with the semiempirical P(Harm) predictions based on Equations (1) and (2) (Table 2).

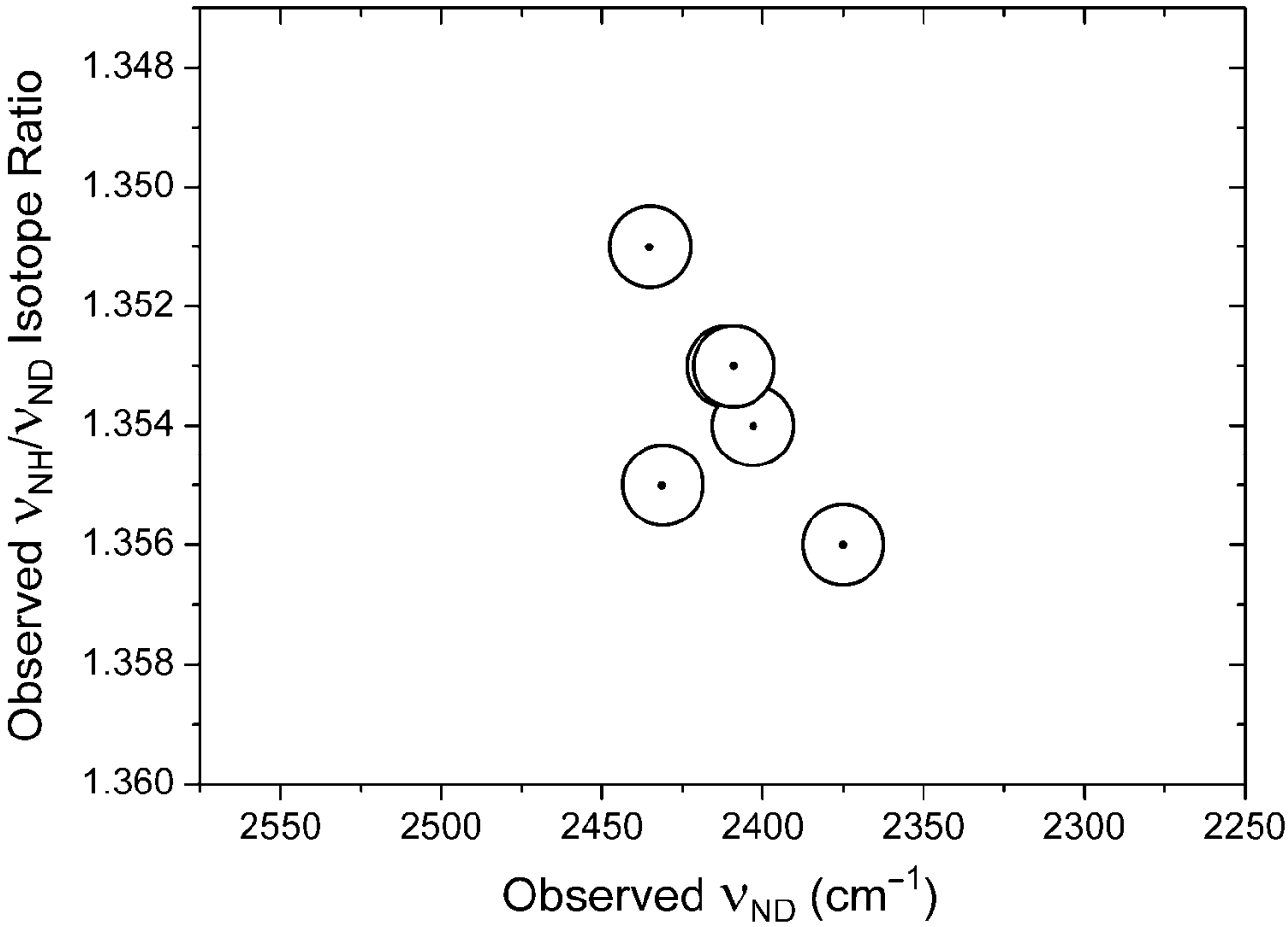

Figure 5. Observed isotope ratios ν_{NH}/ν_{ND} against observed ND stretching wavenumbers ν_{ND} (cm^{-1}) for the esters **16, 17, 19, 20**, and **21** (see Table 3). The data point (2375, 1.356) is from Ref. [55].

In order to establish useful correlations between observed and theoretical NH stretching wavenumbers ν_{NH}, it is crucial to have reliable experimental assignments. Correlations between ν_{NH} and the NH proton chemical shift δ_{NH} have been demonstrated by Dudek [7] and by Gilli et al. [38]. A criterion for including data in the correlation analyses could therefore be that the experimental NH stretching wavenumbers should be consistent with the general correlation between experimental NH stretching frequencies and experimental NH chemical shifts. The plot of ν_{NH} wavenumbers vs. δ_{NH} chemical shifts is shown in Figure 2. The correlation is non-linear, in contrast to the linear relationship obtained for a range of related systems by Dudek [7]. Probably the extension of the range of compounds to include species of the types H, J, and L has led to the non-linear correlation. However, the points for **25** and **26** are striking outliers, and the wavenumbers for these compounds are not included in the correlation analyses. The δ_{NH} values reported [38] for these nitroso derivatives are exceptionally large (Table 2). The reason for the deviation from the correlation curve could be anisotropy effects, such contributions have recently been investigated in similar compounds [56]. Tautomerism could be another reason for a poor fit; deuterium isotope effects on ^{13}C chemical shifts are good tests for tautomerism [57]. Derivatives of 4-amino-3-pentene-2-one (APO), linear and cyclic enaminones, and lactones have been shown to be non-tautomeric [39]. Some enaminones, esters, and lactones may exist both as *E* and *Z* forms; the assumed configurations of the investigated compounds are indicated in Table 1.

It is apparent that structure plays a great role in determining the NH stretching frequencies. The plot in Figure S16 shows a very tight correlation between ν_{NH} and the calculated NH bond length. In general, the NH stretching wavenumbers will depend on the strength of the hydrogen bond. The correlation of observed wavenumbers with the hydrogen bond strengths estimated by the Espinosa method [58] leads to SD = 64–76 cm^{-1}, depending on the choice of fitting function (Figures S17 and S18).

In the following, we discuss a number of literature data using the established correlation equations relating observed and calculated NH stretching wavenumbers (Equations (1) and (2)). A characteristic example is 4-(methylamino)pent-3-en-2-one (**12**). For the observed NH stretching wavenumber, Dudek [7] reported 3100 cm^{-1}, while Raissi et al. [9] reported 3171 cm^{-1}, and Kidwai et al. [8] assigned a feature at 3263 cm^{-1}. As indicated by the P(Harm) values listed in Table 2, Equations (1) and (2) predict 3188 and 3183 cm^{-1} for **12**, pointing to the value 3171 cm^{-1} published by Raissi et al. [9].

Kidwai et al. [8] have published IR data for several β-enaminones. For (*Z*)-4-(phenylamino)pent-3-en-2-one (**6**) and (*Z*)-4-(*p*-nitrophenylamino)pent-3-en-2-one, they reported NH stretching wavenumbers equal to 3000 and 3362 cm^{-1}, respectively. These assignments imply that the substitution of a nitro group in the *para* position of the *N*-phenyl ring of **6** shifts the NH stretching wavenumber by more than 300 cm^{-1}. For the *p*-nitro derivative, we obtain with B3LYP/6-311++G(d,p) and B3LYP/6-31G(d) the harmonic wavenumbers 3229 and 3247 cm^{-1}, respectively, leading to the P(Harm) predictions 3051 and 3063 cm^{-1}. The present predictions indicate that the wavenumber 3362 cm^{-1} published by Kidwai et al. for (*Z*)-4-(*p*-nitrophenylamino)pent-3-en-2-one is much too large.

A number of other discrepancies are found in the literature. A large one is found for the compounds of D type (R = substituted phenyl), **23** and **24**. Gilli et al. [38] report NH stretching frequencies close to 2600 cm^{-1}, whereas Benkheira and Amari [59] report 3390 cm^{-1}. Benkheira and Amari discussed the possibility of a tautomeric equilibrium and concluded that the NH form is dominant, as is also assumed by Gilli et al. The NH chemical shifts are 15.6–15.9 ppm. Hence, the NH stretching frequency 3390 cm^{-1} reported by Benkheira and Amari seems much too high; the correlation in Figure 2 suggests wavenumbers around 2600 cm^{-1}. This prediction is consistent with the semiempirical P(Harm) values (Table 2). Hence, the solid-state value reported by Gilli et al. [38] close to 2600 cm^{-1} seems realistic.

As mentioned above, the experimental wavenumbers for **25** and **26** are not included in the correlation analyses. The latter compound differs from the former only in the substitution of a methoxy group in the *meta* position of the *N*-phenyl ring, which is twisted out of the plane. Very similar NH stretching wavenumbers were computed and predicted for the two compounds (Table 2). However, the reported wavenumber for **26** is 220 cm^{-1} lower than that of **25** [38], a difference that seems hard to explain. Unfortunately, the IR spectra of the two compounds were not published.

Kolev and Angelov [60] investigated 1,1,1-trichloro-3-(1-phenethylamino-ethylidene)-pentane-2,4-dione (Scheme 1, Type A: R_1 = (C=O)CCl_3, R_2 = CH_3, R_3 = CH_2CH_2Ph, X = CH_3). They assigned the observed IR spectrum to the *E* configuration and reported ν_{NH} = 3414 cm^{-1} in the solid state and δ_{NH} = 12.03 ppm. These values yield a point far from the correlation line in Figure 2. With δ_{NH} = 12.03 ppm, the correlation equation in Figure 2 predicts ν_{NH} = 3127 cm^{-1}, indicating a relatively strong hydrogen bond. With B3LYP/6-311++G(d,p) and B3LYP/6-31G(d), we obtain harmonic NH stretching wavenumbers equal to 3272 and 3286 cm^{-1}, respectively. With these values, Equations (1) and (2) predict 3106 and 3117 cm^{-1}, consistent with the value indicated by correlation with the δ_{NH} value. Unfortunately, Kolev and Angelo [59] did not publish this region of the experimental spectrum.

An NH stretching frequency of 3317 cm^{-1} was recently reported for ethyl 2-(benzylamino) cyclopent-1-encarboxylate [36]. Our B3LYP/6-311++G(d,p) and B3LYP/6-31G(d) calculations yield 3451 and 3440 cm^{-1}, respectively. This leads to P(Harm) values equal to 3271 and 3271 cm^{-1}, in fair agreement with the experimental result.

The NH stretching wavenumbers for **27**, **30**, and **31** have apparently not been determined, but δ_{NH} values close to 13.3, 8.84, and 10.26 ppm have been published (Table 2) [7,39–41]. On the basis of the correlation in Figure 2, ν_{NH} values equal to 3007, 3295, and 3238 cm^{-1} can be estimated, respectively, in satisfactory consistency with the predicted P(Harm) values listed in Table 2.

In a number of papers [8,31,35,43,55], enaminones have been studied, but the NH stretching frequencies have not been assigned for all compounds. P(Harm) values predicted with Equations (1) and (2) may be of help in analyzing these spectra.

5. Conclusions

In this work, we considered NH stretching wavenumbers for a large number of species with intramolecular NH···O hydrogen bonding, ranging from weakly to strongly bonded systems. Additionally, a few systems with no intramolecular hydrogen bonding were included. The assignment of the NH stretching bands for a number of compounds was supported by measurements of the ND stretching wavenumbers of the deuterated species. The assignments were also supported by consideration of the correlation between observed NH stretching wavenumber and NH proton chemical shift. This correlation was well described by an exponential function (SD = 34 cm^{-1}), in contrast to the linear relationships found in the literature for related systems.

Excellent exponential relationships were also established between observed NH stretching wavenumbers and harmonic wavenumbers predicted by B3LYP/6-31G(d) and B3LYP/6-311++G(d,p) calculations. With SD = 38 cm^{-1}, these semiempirical correlation equations should be of considerable predictive value, as demonstrated in the Discussion Section of this article (Section 4). This result is significant because rigorous theoretical procedures exceeding the harmonic approximation, such as the VPT2 procedure, tend to be impractical for large molecules, requiring orders of magnitude more computing time than the harmonic analysis.

The non-linearity of these relationships is in contrast to previous results for OH···O systems, which were characterized by corresponding linear relationships. We have presently no obvious explanation for the apparent difference between NH···O and OH···O systems. NH stretching wavenumbers computed with the anharmonic VPT2 approximation are found to be linearly related to the corresponding harmonic values, offering no explanation of the non-linearity of the present correlations. It would seem that more advanced theoretical calculations, beyond the VPT2 approximation, are called for.

Supplementary Materials: The following are available online, Figures S1–S11: IR spectra; Figures S12–S18: Correlation analyses; Figures S19 and S20: Detailed results for (*Z*)-ethyl 3-(methylamino)but-2-enoate (**17**); Figure S21: Materials section with synthesis, characterization and NMR spectra.

Author Contributions: Conceptualization, methodology, investigation, formal analysis, writing—original draft preparation, writing—review and editing, P.E.H.; investigation, formal analysis, writing—review and editing, M.V.; investigation, writing—review and editing, F.S.K.; conceptualization, methodology, investigation, formal analysis, visualization, writing—original draft preparation, writing—review and editing, J.S.-L. All authors have read and agreed to the published version of the manuscript.

Funding: This work was supported by Ferdowsi University of Mashhad, Iran, providing sabbatical time for Mohammad Vakili at Roskilde University, Denmark.

Institutional Review Board Statement: Not applicable.

Informed Consent Statement: Not applicable.

Data Availability Statement: Not applicable.

Acknowledgments: The authors wish to thank Eva Marie Karlsen for her help in recording IR spectra.

Conflicts of Interest: The authors declare no conflict of interest.

References

1. Hansen, P.E. Review: A Spectroscopic Overview of Intramolecular Hydrogen Bonds of NH . . . O,S,N Type. *Molecules* **2021**, *26*, 2409. [CrossRef] [PubMed]
2. Pimentel, G.C.; McClellan, A.L. *The Hydrogen Bond*; W.H. Freeman: San Francisco, CA, USA, 1960.
3. Vinograd, S.N.; Linnell, R.H. *Hydrogen Bonding*; Van Nostrand Reinhold: New York, NY, USA, 1971.
4. Joesten, M.D.; Schaad, L.J. *Hydrogen Bonding*; Marcel Dekker: New York, NY, USA, 1974.
5. Arunan, E.; Desiraju, G.R.; Klein, R.A.; Sadlej, J.; Scheiner, V.; Alkorta, I.; Clary, D.C.; Crabtree, R.H.; Dannenberg, J.J.; Hobza, P.; et al. Definition of the hydrogen bond (IUPAC Recommendation 2011). *Pure Appl. Chem.* **2011**, *83*, 1537–1641. [CrossRef]
6. Tayyari, S.F.; Zeegers-Hyuskens, T.; Wood, J.L. Spectroscopic study of hydrogen bonding in the enol form of β-diketones—II. Symmetry of the hydrogen bond. *Spectrochim. Acta A* **1979**, *35*, 1289–1295. [CrossRef]
7. Dudek, G.O. Spectroscopic Studies of Keto—Enol Equilibria. VIII. Schiff Base Spectroscopic Correlations. *J. Org. Chem.* **1965**, *30*, 548–552. [CrossRef]
8. Kidwai, M.; Bhardwaj, S.; Misshra, N.K.; Bansal, V.; Kumar, A.; Mozumdar, S. A novel method for the synthesis of β-enaminones using Cu-nanoparticles as catalyst. *Catal. Commun.* **2009**, *10*, 1514–1517. [CrossRef]
9. Raissi, H.; Moshfeghi, E.; Farzad, F. Vibrational assignment, structure and intramolecular hydrogen bond of 4-methylamino-3-penten-2-one. *Spectrochim. Acta A* **2005**, *62*, 1004–1015. [CrossRef]
10. Hansen, B.K.V.; Winther, M.; Spanget-Larsen, J. Intramolecular hydrogen bonding. Spectroscopic and theoretical studies of vibrational transitions in dibenzoylmethane enol. *J. Mol. Struct.* **2006**, *790*, 74–79. [CrossRef]
11. Hadži, D. (Ed.) *Theoretical Treatment of Hydrogen Bonding*; Wiley: Chichester, UK, 1997.
12. Ferrari, B.C.; Bennett, C.J. A Comparison of Medium-Sized Basis Sets for the Prediction of Geometries, Vibrational Frequencies, Infrared Intensities and Raman Activities for Water. *J. Phys. Conf. Ser.* **2019**, *1290*, 012013. [CrossRef]
13. Foresman, J.B.; Frisch, A.E. *Exploring Chemistry with Electronic Structure Methods*, 3rd ed.; Gaussian, Inc.: Wallingford, CT, USA, 2015.
14. Scott, A.P.; Radom, L. Harmonic Vibrational Frequencies: An Evaluation of Hartree-Fock, Møller-Plesset, Quadratic Configuration Interaction, Density Functional Theory, and Semiempirical Scale Factors. *J. Phys. Chem.* **1996**, *100*, 16502–16513. [CrossRef]
15. Wong, M.W. Vibrational frequency prediction using density functional theory. *Chem. Phys. Lett.* **1996**, *256*, 391–399. [CrossRef]
16. Becke, A.D. Perspective: Fifty years of density-functional theory in chemical physics. *J. Chem. Phys.* **2014**, *140*, 18A301. [CrossRef] [PubMed]
17. Becke, A.D. Density functional thermochemistry. III. The role of exact exchange. *J. Chem. Phys.* **1993**, *98*, 5648–5652. [CrossRef]
18. Lee, C.; Yang, W.; Parr, R.G. Development of the Colle-Salvetti correlation-energy formula into a functional of the electron density. *Phys. Rev. B.* **1988**, *37*, 785–789. [CrossRef]
19. Perdew, J.P.; Wang, Y. Accurate and simple analytic representation of the electron gas correlation energy. *Phys. Rev. B* **1992**, *45*, 13244–13249. [CrossRef]
20. Spanget-Larsen, J.; Hansen, B.K.V.; Hansen, P.E. OH stretching frequencies in systems with intramolecular hydrogen bonds. Harmonic and anharmonic analyses. *Chem. Phys.* **2011**, *389*, 107–115. [CrossRef]
21. Hansen, P.E.; Spanget-Larsen, J. Prediction of OH Stretching frequencies in systems with intramolecular hydrogen bonds. *J. Mol. Struct.* **2012**, *1018*, 8–13. [CrossRef]
22. Barone, V. Anharmonic vibrational properties by a fully automated second order pertubative approach. *J. Chem. Phys.* **2005**, *122*, 14108. [CrossRef]
23. Barone, V.; Biczysko, M.; Bloino, J. Fully anharmonic IR and Raman spectra of medium-size molecular systems: Accuracy and interpretation. *Phys. Chem. Chem. Phys.* **2014**, *16*, 1759–1787. [CrossRef] [PubMed]
24. Hansen, P.E.; Spanget-Larsen, J. Review: NMR and IR Investigations of Strong Intramolecular Hydrogen Bonds. *Molecules* **2017**, *22*, 552. [CrossRef]
25. Hansen, P.E.; Jezierska, A.; Panek, J.; Spanget-Larsen, J. Theoretical Calculations Are a Strong Tool in the Investigation of Strong Intramolecular Hydrogen Bonds. In *Molecular Spectroscopy: A Quantum Chemistry Approach*; Ozaki, Y., Wójcik, M.J., Popp, J., Eds.; Wiley-VCH: Weinheim, Germany, 2019; Volume 1, Chapter 8; pp. 215–251.
26. Dabrowski, J. IR Spectra and Structure of substituted unsaturated Carbonyl compounds. X. β-alkylaminoacroleins. *J. Mol. Struct.* **1969**, *3*, 227–233. [CrossRef]
27. Dabrowski, J.; Dabrowska, U. Infrarotspektren und Struktur substituierter ungesättigter Carbonylverbindungen, VII. Enaminoketone mit starrer *s-cis*- und *s-trans*-Konformation und sekundär Aminogruppe. *Chem. Ber.* **1968**, *101*, 2365–2374. [CrossRef]
28. Vdovenko, S.I.; Gerus, I.I.; Pagacz-Kostrzewa, M.; Wierzejewska, M.; Zhuk, Y.I.; Kukhar, V.P. Special feature of kinetics of ZcE isomerisation of β-*N*-methylaminovinyl trifluoromethyl ketone in Ar matrix exposed to UV radiation and spontaneous E⇆Z isomerization of α-methyl-β-*N*-methylaminovinyl trifloromethyl ketone. *Spectrochim. Acta A* **2018**, *199*, 130–140. [CrossRef]
29. Vdovenko, S.I.; Gerus, I.I.; Zhuk, Y.I.; Kukhar, V.P.; Pagacz-Kostrzewa, M.; Wierzejewska, M.; Daniluc, C.-G. The conformation analysis of push-pull enaminones using FTIR and NMR spectroscopy and quantum mechanical calculations.VI. 4-*N*-Methylaminovinyl trifluoromethyl ketone and 3-methyl-2-*N*-methylaminovinyl trifluoromethyl ketone. *J. Mol. Struct.* **2017**, *1128*, 741–753. [CrossRef]
30. Chiara, J.L.; Gómez-Sánchez, A.; Bellanato, J. Spectral properties and isomerism of nitroenamines. Part 4. β-Amino-α-nitro-α,β-unsaturated ketones. *J. Chem. Soc. Perkin Trans. 2* **1998**, *8*, 1797–1806. [CrossRef]

31. Das, B.; Venkateswarly, K.; Majhi, A.; Reddy, M.R.; Reddy, K.N.; Rao, Y.K.; Ravikumar, K.; Sridhar, B. Highly efficient, mild and chemo- and stereoselective synthesis of enaminones and enamino esters using silica supported perchloric acid under solvent-free conditions. *J. Mol. Catal. A* **2006**, *246*, 276–281. [CrossRef]
32. Patil, S.A.; Gonzalez-Flores, D.; Medina, P.A.; Dever, S.; Stentzel, M.; Popp, J.; Pineda, L.W.; Montero, M.L.; Ziller, J.W.; Fahlman, B.D. Synthesis, Characterization and Crystal Structure of (*Z*)-3-(4-Chlorophenylamino)-1-Phenylbut-2-En-1-One. *J. Chem. Crystallogr.* **2012**, *42*, 543–548. [CrossRef]
33. Zheglova, D.K.; Genov, D.G.; Bolvig, S.; Hansen, P.E. Deuterium Isotope Effects on ^{13}C Chemical Shifts of Enaminones. *Acta Chem. Scand.* **1997**, *51*, 1016–1023. [CrossRef]
34. Chipanina, N.N.; Oznobikhina, L.P.; Aksamentova, T.N.; Romanov, A.R.; Rulev, A.Y. Intramolecular hydrogen bond in the push-pull CF_3-aminoenones: DFT and FTIR study, NBO analysis. *Tetrahedron* **2014**, *70*, 1207–1213. [CrossRef]
35. Chen, X.; She, J.; Shang, Z.; Wu, J.; Wu, H.; Zhang, P. Synthesis of Pyrazoles, Diazepines, Enaminones, and Enamino Esters using 12-Tungstophosporic Acid as a Reusable Cata-lyst in Water. *Synthesis* **2008**, *21*, 3478–3486.
36. Wang, D.; Zhang, L.; Luo, S. Visible Light Promoted β-C–H Alkylation of β-Ketocarbonyls via a β-Enaminyl Radical Intermediate. *Chin. J. Chem.* **2018**, *36*, 311–320. [CrossRef]
37. Sánchez, A.G.; Valle, A.M.; Bellanato, J. Infrared Absorption and Isomerism of 3-Aminocrotonic Esters. Part I. 3-(Alkylamino)crotonic Esters. *J. Chem. Soc. B: Phys. Org.* **1971**, 2330–2335. [CrossRef]
38. Gilli, P.; Bertolasi, V.; Ferretti, V.; Gilli, G. Evidence for Intramolecular N-H···O Resonance-Assisted Hydrogen Bonding in β-Enaminones and Related Heterodienes. A Combined Crystal-Structural, IR and NMR Spectroscopic, and Quantum-Mechanical Investigation. *J. Am. Chem. Soc.* **2000**, *122*, 10405–10417. [CrossRef]
39. Hansen, P.E.; Bolvig, S.; Duus, F.; Petrova, M.V.; Kawecki, R.; Krajewski, R.; Kozerski, L. Deuterium Isotope Effects on ^{13}C Chemical Shifts of Intramolecular Hydrogen-Bonded Olefins. *Magn. Reson. Chem.* **1995**, *33*, 621–631. [CrossRef]
40. Štefane, B.; Polanc, S. A new and a convenient route to enaminones and pyrazoles. *New J. Chem.* **2002**, *26*, 28–32. [CrossRef]
41. Valduga, C.J.; Squizani, A.; Braibante, H.S.; Braibante, M.E.F. The Use of K-10/Ultrasound in the Selective Synthesis of Unsymmetrical β-Enamino Ketones. *Synthesis* **1998**, 1019–1022. [CrossRef]
42. Koduri, N.D.; Hileman, B.; Cox, J.D.; Scott, H.; Hoang, P.; Robbins, A.; Bowers, K.; Tsebaot, L.; Miao, K.; Castaned, M.; et al. Acceleration of the Eschenmoser coupling reaction by sonication: Efficient synthesis of enaminones. *RSC Adv.* **2013**, *3*, 181–188. [CrossRef]
43. Célérier, J.-P.; Deloisy, E.; Hommet, G.L.; Maittte, P. Lactim Ether Chemistry. Cyclic β-Enamino Ester Synthesis. *J. Org. Chem.* **1979**, *44*, 3089. [CrossRef]
44. Ullah, S.; Zhang, W.; Hansen, P.E. Deuterium Isotope Effects on ^{13}C and ^{15}N Chemical Shifts of Intramolecularly Hydrogen-Bonded β-Enamine Derivatives of Meldrum's and Tetronic acid. *J. Mol. Struct.* **2010**, *976*, 377–391. [CrossRef]
45. Balogh, M.; Laszlo, P.; Simon, K. Unusual Reactions between 1,4-Dihydropyridines and 1,2,4,5-Tetrazines in the Presence of K-10/Fe(III) Clay Catalyst. *J. Org. Chem.* **1987**, *52*, 2026–2029. [CrossRef]
46. Petrova, M.; Muhamadejev, R.; Vigante, B.; Duburs, G.; Liepinsh, E. Intramolecular hydrogen bonds in 1,4-dihydropyridine derivatives. *R. Soc. Open. Sci.* **2018**, *5*, 180088. [CrossRef]
47. Darugar, V.; Vakili, M.; Tayyari, S.F.; Hansen, P.E.; Kamounah, F.S. Molecular structure, intramolecular hydrogen bond strength, vibrational assignment, and spectroscopic insight of 4-phenylamino-3-penten-2-one and its derivatives: A theoretical and experimental study. *J. Mol. Liq.* **2021**, *334*, 116035. [CrossRef]
48. Seyedkatouli, S.; Vakili, M.; Tayyari, S.F.; Hansen, P.E.; Kamounah, F.S. Molecular structure and intramolecular hydrogen bond strength of 3-methyl-4-amino-3-penten-2-one and its N-Me and N-Ph substitutions by experimental and theoretical methods. *J. Mol. Struct.* **2019**, *1184*, 233–245. [CrossRef]
49. Frisch, M.J.; Trucks, G.W.; Schlegel, H.B.; Scuseria, G.E.; Robb, M.A.; Cheeseman, J.R.; Scalmani, G.; Barone, V.; Mennucci, B.; Petersson, G.A.; et al. *Gaussian 09*; Revision D.01; Gaussian, Inc.: Wallingford, CT, USA, 2009.
50. Frisch, M.J.; Trucks, G.W.; Schlegel, H.B.; Scuseria, G.E.; Robb, M.A.; Cheeseman, J.R.; Scalmani, G.; Barone, V.; Petersson, G.A.; Nakatsuji, H.; et al. *Gaussian 16*; Revision A.03; Gaussian, Inc.: Wallingford, CT, USA, 2016.
51. Biegler-König, F.W.; Schönbohm, J.; Bayles, D. Software news and updates—AIM2000—A program to analyze and visualize atoms in molecules. *J. Comp. Chem.* **2001**, *22*, 545–559.
52. Mroginski, M.-A.; Németh, K.; Bauschlicher, T.; Klotzbücher, W.; Goddard, R.; Heinemann, O.; Hildebrandt, P.; Mark, F. Calculation of Vibrational Spectra of Linear Tetrapyrroles. 3. Hydrogen-Bonded Hexamethylpyrromethene Dimers. *J. Phys. Chem. A* **2005**, *109*, 2139–2150. [CrossRef]
53. Novak, A. Hydrogen Bonding in Solids, Correlation of Spectroscopic and Crystallographic Data. *Struct. Bond.* **1974**, *18*, 177–216.
54. Sobczyk, L.; Obrzud, M.; Filarowski, A. H/D Isotope Effects in Hydrogen Bonded Systems. *Molecules* **2013**, *18*, 4467–4476. [CrossRef] [PubMed]
55. Rodríguez, M.; Santillan, R.; López, Y.; Farrán, N.; Barba, V.; Nakatani, K.; García-Baéz, E.V.; Padilla-Martínez, I.I. N–H·O Assisted Structural Changes Induced on Ketoenamine Systems. *Supramol. Chem.* **2007**, *19*, 641–653. [CrossRef]
56. Hansen, P.E.; Koch, A.; Kleinpeter, E. Ring Current and Anisotropy Effects on OH Chemical Shifts. *Tetrahedron Lett.* **2018**, *59*, 22188–22192. [CrossRef]
57. Hansen, P.E. Isotope Effects on Chemical Shifts of Hydrogen Bonded Systems. *J. Label. Comp. Radiopharm.* **2007**, *50*, 967–981. [CrossRef]

58. Espinosa, E.; Molins, E.; Lecomte, C. Hydrogen bond strengths revealed by topological analyses of experimentally observed electron densities. *Chem. Phys. Lett.* **1998**, *285*, 170–173. [CrossRef]
59. Benkheira, F.Z.; Amari, M. Etude Spectroscopique de l'équilibre enaminone—Iminenol de la reaction de l'acide dehydroacetique avec les amines primaires. *J. Mar. Chim. Heterocycl.* **2016**, *15*, 85–91.
60. Kolev, T.M.; Angelov, P. 1,1,1-Trichloro-3-(1-phenethylamino-ethylidene)-pentane-2,4-dione—Synthesis, spectroscopic, theoretical and structural elucidation. *J. Phys. Org. Chem.* **2007**, *20*, 1108–1113. [CrossRef]